Marine Pollution Bulletin 159 (2020) 111485

Contents lists available at ScienceDirect

Marine Pollution Bulletin

journal homepage: www.elsevier.com/locate/marpolbul

Fate and behaviour of weathered oil drifting into sea ice, using a novel wave and current flume

Ivar Singsaas[a,*], Frode Leirvik[a], Per S. Daling[a], Chantal Guénette[b], Kristin Rist Sørheim[a]

[a] SINTEF Ocean AS, P.O. box 4762, Torgard, NO-7465 Trondheim, Norway
[b] ECRC~SIMEC, 1201 – 275 Slater Street, Ottawa K1P 5H9, Canada

ARTICLE INFO

Keywords:
Fate and behaviour
Flume experiments
Oil spill
Arctic
Ice
Weathering

ABSTRACT

Increased knowledge about the fate and behaviour of weathered oil in different sea ice conditions is essential for our ability to model oil spill trajectories in ice more precisely and for oil spill response decision making in northern and Arctic areas. As part of the 3-year project: "Fate, Behaviour and Response to Oil Drifting into Scattered Ice and Ice Edge in the Marginal Ice Zone", a novel wave and current flume was built to simulate these processes in the laboratory. This paper discusses some of the findings from this project, which included Marine Gas Oil and four Norwegian crude oils. All crude oils were weathered prior to testing, simulating having drifted on the sea surface for a period (tentatively 1–3 days) before encountering ice. The build-up of oil drifting against an ice barrier and horizontal and vertical migration of oil droplets under solid ice and in frazil ice was studied.

1. Introduction

Oil exploration activities have been ongoing for many years in the Norwegian Arctic, mainly in the Barents Sea area. New oil exploration blocks are located in areas where open water conditions are expected throughout most of the year. However, during the winter seasons there is the risk for an oil spill to drift towards a solid ice barrier or areas with scattered or frazil ice. Similar challenges are seen for other circumpolar areas with petroleum activities, for instance offshore Newfoundland and Labrador (NL) in Canada. The dynamic ice situation in these areas is characterized by ice front movements, based on the prevailing environmental conditions (e.g. wind and currents) and other local factors.

In 2006, a 4-year SINTEF led Joint Industry Program (JIP) on "Oil Spill Contingency for Arctic and Ice-covered Waters" was initiated (https://www.sintef.no/projectweb/jip-oil-in-ice/) (Sørstrøm et al., 2010). Laboratory, basin and field studies of five very different oil types indicated that the rate of weathering processes (e.g. evaporation and water uptake) and change in physicochemical properties (e.g. viscosity of w/o emulsions, density, pour point etc.) taking place if the oils are spilt into sea, is very dependent on oil composition, energy and ice conditions (Brandvik and Faksness, 2009; Brandvik et al., 2010). Experiments demonstrated that in open water, weathering processes generally occur more rapidly, resulting in a faster increase in viscosity and density, compared to experiments performed in 50 and 90% ice. In ice, the oil generally weathers more slowly which may extend the window of opportunity for using some oil spill response strategies.

In 2012 a second JIP on "Arctic Oil Spill Response Technology" was initiated by the International Association of Oil & Gas Producers (IOGP) to undertake specifically targeted research and technology projects to further improve Arctic spill response capabilities (Dickins, 2017) (http://www.arcticresponsetechnology.org/). The IOGP JIP focussed on different response technologies, environmental effects, trajectory modelling and remote sensing. It was concluded that the choice of optimal oil spill response options in the Arctic can vary greatly depending on many factors, for example location, timing, ice conditions, ice season duration, environmental sensitivities, and oil properties. According to Dickins (2017), the current generation of oil spill models could predict the behaviour of oil and its likely fate in ice environments (e.g. degree of evaporation, rate of emulsification, etc.), but at the outset of the JIP in 2012, they had limited capabilities to model oil movements in the presence of a significant ice cover. This deficiency resulted from a combination of the limited resolution offered by the existing ice models, and the inability of the existing oil spill trajectory models to import and process data from ice models.

There has been much focus on the importance of ice coverage for the behaviour of oil in ice. Venkatesh et al. (1990) suggested that for low ice concentrations (less than 30%) oil behaved as in open water. For oil concentrations above 70–80% they found that the oil drifts with the ice, while for 30 to 70% ice concentration there would be variations in oil behaviour and more research was needed. Ice exists in a wide

* Corresponding author.
E-mail address: Ivar.Singsaas@sintef.no (I. Singsaas).

https://doi.org/10.1016/j.marpolbul.2020.111485
Received 24 February 2020; Received in revised form 11 July 2020; Accepted 13 July 2020
Available online 04 August 2020

variety of ice types, morphologies, and characteristics like thickness, degree of coverage, floe size, porosity, and so forth. During an oil spill in ice covered waters, the oil may be dispersed and trapped under ice. The fate and behaviour of this oil depends on several different factors (CJ Beegle-Krause et al., 2013) like e.g.: under-ice roughness, concentration and consolidation of the ice pack, dampening of waves due to ice cover and distance from the ice edge, under-ice currents, and freezing of oil into the ice.

If oil is released below the ice cover, from a sunken vessel, pipeline rupture or a well blowout, the oil may be broken down into small droplets as it rises through the water column (Johansen et al., 2013). However, in case of a blowout most of the oil droplets will coalesce to form an oil slick when they reach the underside of the ice (Wilkinson et al., 2017). The rate at which oil spreads under sea ice is influenced by the rate at which the oil is introduced, the oil viscosity, and the oil-ice-water interfacial tensions, while oil movement under ice is dominated by the under-ice roughness (e.g. Wilkinson et al., 2007).

If the density of oil is lower than the surrounding sea water, the oil will attempt to migrate upwards into the sea ice. This migration is limited when the ice is cold. The oil uptake capacity of the lower ice skeletal layers has been studied by several scientists including: Karlsson et al. (2011), Petrich et al. (2013), and Wilkinson et al. (2007). Studies indicate that oil under or encapsulated within sea ice will be released as the ice warms up. The release will be either through vertical migration of oil or through melting of the ice surface downwards (e.g. Dickins, 2011). Literature on horizontal and vertical movement of oil in frazil or slush-like ice is more limited. However, Wilkinson et al. (2014) reported basin experiments studying oil movement under sea ice. A fresh crude oil was tested on three ice types: frazil ice, nilas, and pancake ice.

Research on oil fate and behaviour in ice has to a large degree focussed on fresh crude oils. Oil released in open water that drift for some time before encountering the ice, will have reached a certain degree of weathering, depending the oil type, weather conditions and drift time. The fate and behaviour of weathered oils drifting into a solid ice barrier, scattered or frazil ice conditions is not well understood. The oil may be contained at the sea surface against an ice barrier, may accumulate creating a thick layer, or may be pushed under or over the ice under certain wave conditions. Depending on the oil type, the degree of weathering and ice characteristics, some oils may be retained by the ice while others might migrate into ice or easily be washed off the ice. All these behaviours will influence the efficiency of different response methods: the use of dispersants and in-situ burning (ISB) have gained interest as a supplement or an alternative to mechanical recovery for an oil spill in ice.

To address some of the knowledge gaps related to the interaction of weathered oils in different ice conditions, a 3-year project was initiated by SINTEF with the support of the Research Council of Norway (NRC) and the oil industry (the FateIce project). It was based on the understanding that more fundamental knowledge about the fate and behaviour of oil drifting into solid ice, scattered or frazil ice conditions is required in order to modify and customize response technologies and improve tools for 3-D oil spreading and response modelling of oil spill scenarios in ice. Such knowledge will be important for:

- The oil industry and public responders to develop improved operational procedures for oil spill contingency and response.
- Oil spill response equipment manufacturers in the development of more efficient technology.
- Research organisations and consultants to provide improved and more detailed simulations of oil spill trajectories, effect of response options, and spill impact mitigation assessment (SIMA).
- Public agencies to develop appropriate regulations for oil spill contingency.
- Design of reliable future bioassay studies on relevant species and field validation studies in ice.

Fig. 1. A picture of an area with frazil ice mixed with “pancake” ice from the Norwegian part of the Barents Sea.
Photo: NOFO/BaSEC 2015.

Two different ice scenarios were selected as a basis for the experiments performed in this project: solid ice and frazil ice. A solid ice barrier would represent closely packed large ice floes or a long continuous barrier of ice, into which weathered oil could be accumulated and confined with a low potential to penetrate the ice. The other ice scenario is referred to as frazil ice. It represents recently formed ice composed of ice crystals which are only weakly frozen together and is in literature also often referred to as grease ice (World Meteorological Organization, 1970; Smedsrud and Skogseth, 2005; Martin and Kauffman, 1981). For the purpose of this paper, the term frazil ice is used to describe this scenario. Fig. 1 shows a photo of an area in the Barents Sea covered with this ice type mixed with “pancake” ice.

2. Objectives

The overall objective of the FateIce (“Fate, Behaviour and Response to Oil Drifting into Scattered Ice and Ice Edge in the Marginal Ice Zone (MIZ)”) project was:

- To provide new knowledge of oil's fate and behaviour when drifting into a solid ice barrier or scattered ice conditions as a foundation for establishing robust oil spill response technologies, strategies, and operations for such spill scenarios.

Secondary objectives for the wave and current flume experiments:

- Increased understanding of processes taking place when different oil types with different weathering degrees are meeting the ice.
- Interaction with and distribution of weathered oil in different ice conditions: solid ice barrier, frazil ice, thawing periods.

To meet these objectives, a large number of experiments were performed in a novel wave and current flume using the two ice scenarios described above.

2.1. Solid ice barrier

Two types of experiments were carried out in the solid ice scenario: fate and behaviour of weathered oil as it drifts against a solid barrier and the horizontal movement of oil droplets under a solid ice layer. Experiments carried out to studying the drift of weathered oil against a solid ice barrier were designed with the aim to support development of a simple model to predict the thickness of oil forced against a barrier by a current. Results from these experiments have been used for comparison and validation against output from model predictions (Nordam et al., 2020).

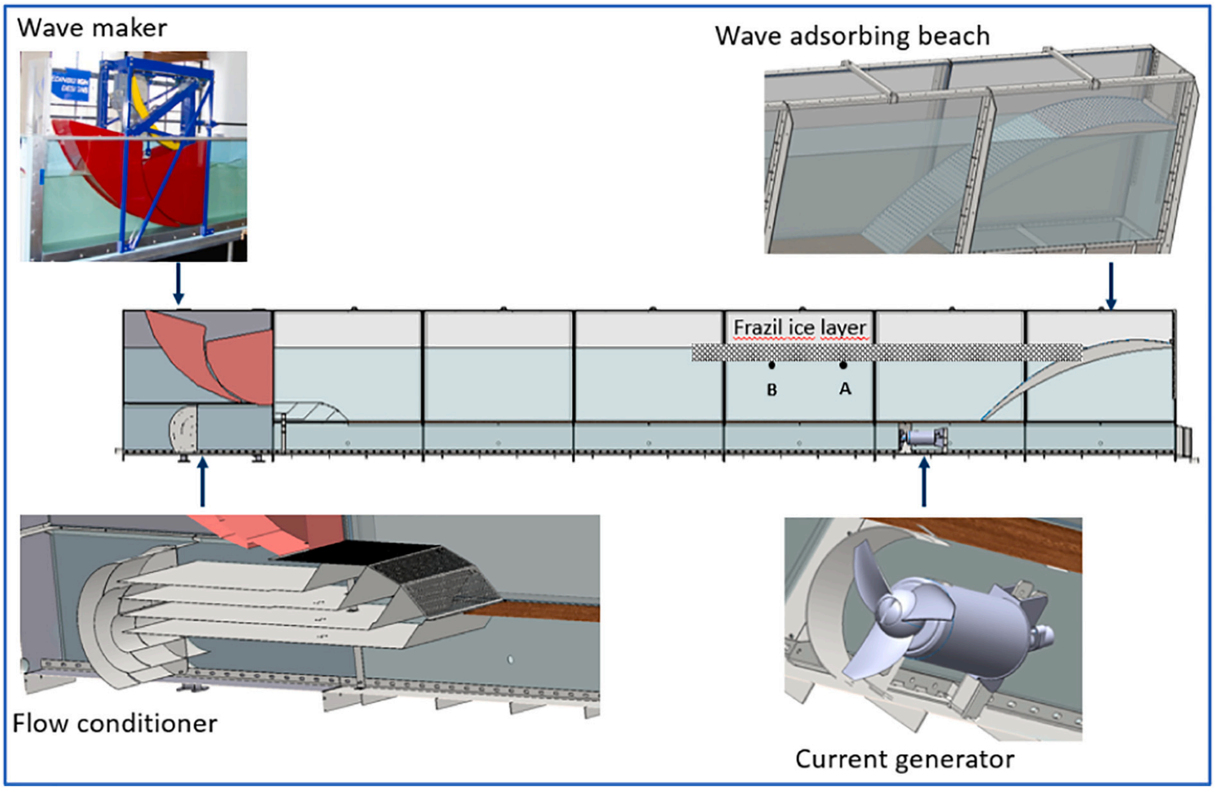

Fig. 2. Sketch of the SINTEF Sealab wave and current flume showing the equipment installed inside the flume. The approximate position of the frazil ice layer used in the experiments is indicated in the figure, with position A and B, 2 and 1 m inside from the leading edge of the ice field, respectively.

2.2. *Frazil ice*

A series of experiments was designed to study the potential for weathered oil to migrate into frazil ice, both horizontally and vertically. Variables studied in these experiments included oil type, degree of weathering, wave regimes and currents.

3. Testing facilities and methods

3.1. *SINTEF Sealab wave and current flume*

A novel wave and current flume was built to perform these experiments (Fig. 2). The following operational properties were implemented in the construction of the flume:

- The 14 meters long flume, with a skeleton in stainless steel, was built with large tempered and laminated glass windows on either side for visual insight.
- A piston type wave-maker (Edinburgh Designs) was selected. By use of a sophisticated computer program the wave-maker created well-defined waves with a variety of wave heights and amplitudes.
- A computer-controlled propeller was installed in the lower compartment (“double bottom”). It produced a water flow that was conditioned by plates and gratings under the wave maker to create a well-defined current.
- The flume could rapidly be filled with 10.5 m^3 filtrated sea water, pumped in from 60 meters depth in the fjord outside the facility.
- The flume was installed in a temperature-controlled room with the possibility to take the temperature down to −18 °C. This was important both for making ice, doing experiments at reproducible low temperatures and to avoid melting of ice between experiments.

The advantage of this flume is the combination of all the operational properties implemented. Besides, this flume was primarily built for experiments with oil. Many similar existing flumes are built for other purposes and cannot be contaminated with oil. The flume proved to work very well in the experiments performed in this project.

To document the spreading and behaviour of oil, two cameras were mounted above the flume. Videos were binarized and stitched together and images analysed to produce a time series of slick behaviour throughout the experiments. To study formation and movement of oil droplets under ice, a combination of a mirror and a camera was used (Fig. 3). The mirror was mounted at a 45° angle under the ice. A SLR (Single Lens Reflex) camera recorded the droplets under the ice at a frame rate of 1 image per second. Images were processed to show drift speed and droplet size. Oil thickness was estimated by combining the volume of oil added with the slick area measured from above. In the experiments studying oil thickness against a solid ice barrier, the thickness varied across the oil layer and the measurements were supplied by images of the slick from the underside to evaluate the shape and the thickness against the barrier. Ice thickness and wave amplitude were manually measured at the glass windows at the side of the flume. Building the flume with large glass windows was advantageous in controlling such parameters.

3.2. *Selection of oils and preparation of oil samples*

The test oils were selected to represent a broad range of physico-chemical properties to reflect the expected range of fate and behaviour of the weathered samples. A prior laboratory weathering study of the oils had been carried out, and the following Norwegian crude oils were identified to meet the requirements: Wisting Central, Troll B, Oseberg Blend and Grane. In addition, a Marine Gas Oil (MGO) was selected as a relevant fuel oil for the Norwegian Arctic.

Because this project was aiming at studying oil-ice interaction after the oil had drifted for some time in open waters, it was necessary to artificially weather the oils before testing. SINTEF has developed procedures for artificial weathering of oils, both in small-scale (e.g. Daling

Fig. 3. Picture of the SLR camera mounted outside the flume window taking pictures from underside the ice through a 45° mirror.

et al., 1990) and larger scale (Ramstad et al., 2008). In this project the oils were evaporated in 200 to 400 l batches in a topping tank. The oil was heated, circulated, and sprayed through a "shower head". Air was blown through the tank and oil vapour was condensed and taken care of in a chamber outside the tank. 250 °C+ residues were prepared for each oil (270 °C+ for the Grane oil) while 200 °C+ residues were prepared for two of the oils. In a 250 °C+ residue all components with boiling point below 250 °C is evaporated off. As a rule of thumb 200 °C+ and 250 °C+ residues are assumed to represent 0.5–1 day and 0.5–1 week of evaporation at sea, respectively. MGO was not evaporated. The composition of the final evaporated residue was verified by gas chromatography. It was compared to the gas chromatogram for fresh oil and for a similar sample evaporated by the small-scale methodology, by looking at the distribution of hydrocarbon peaks (up to nC_{40}). Measurement of density was also used to verify the degree of evaporation of the residue by comparing the measured density to similar small-scale data from previous weathering studies for each oil. Viscosity, pour point, asphaltene and wax contents were also measured for the water-free residues. Table 1 gives an overview of the oils and their physicochemical and emulsion properties. Unless otherwise noted, the viscosities were measured at a temperature of 0 °C. Table 2 gives an overview of the analytical methods and instrumentation used.

Water-in-oil (w/o) emulsions were prepared using a purpose built 20-L tank and pump system. Oil was drawn from the bottom of the tank, circulated through the pump, and reinjected at the top. Water was carefully injected through a valve at the suction side of the pump and mixed with the oil to create an emulsion.

Quality assurance and control of the physicochemical analyses was obtained by using standardized analytical methods and instrumentation (Table 2). The wave and current flume is automated, operated by a computer program. Wave heights and frequencies were measured manually for calibration and verification of the computer settings. Current was calibrated by manual measurements in the flume. Air and water temperatures were measured daily or more often if required.

The preparation of weathered oil samples was done by a methodology developed by SINTEF and which has been used to prepare samples for a large number of previous basin and field experiments. Because this methodology involved evaporation of oil components with low boiling points, a risk analysis and SJA was performed before the work was initiated. PPE was mandatory.

3.3. Preparation of ice

A solid sheet of ice measuring 2 m long by 0.5 m wide by 8 cm thick was prepared using a wooden box located in a cold room at a temperature of −20 °C. A light metal frame was frozen into the ice to facilitate handling. The ice was prepared using water with a salinity of 0.5%. By preparing ice from low salinity water it was possible to create a solid ice barrier with a smooth and hard underside. This ice block was primarily used to study oil thickness against a solid ice barrier but was also used as a base for studying movement of oil droplets under ice. The smooth underside was not representative of the bottom surface of sea ice, which typically will have a softer skeletal layer. Therefore, frazil and skeletal ice were made and placed under this ice block to represent a greater roughness. An advantage of preparing ice from low salinity water was that the ice had a freezing point close to 0 °C whereas the water in the flume was natural sea water with a salinity of 3.5% and freezing point of −1.8 °C. This extended the period that the ice block could be used without melting. The same ice block was used throughout the entire experimental period.

Frazil ice was made from sea water in the flume by lowering the air temperature to between −4 and − 5 °C and running the wave generator at very low speed and amplitude. A 10 to 15 cm thick layer of frazil ice could be produced over a period of one to two days when starting with a sea water temperature at or near its freezing point. Frazil ice is regarded as the first stage of sea ice formation (Wilkinson et al., 2014). The size of frazil ice crystals varies from 1 to 10 mm in seawater.

4. Experimental design

In total, three series of experiments were performed in the solid ice barrier scenario and four series in the frazil ice scenario (Table 3).

This paper focusses on oil thickness against a solid ice barrier (1a in

Table 1
Data from topping and w/o emulsification (50% and 75% of water) of the test oils. Marine Gas Oil (MGO) was not topped or emulsified.

Oil	Residue	Amount residue	Density kg/l	Pour point °C	Asph wt%	Wax wt%	Viscosity			
							Water free 10s^{-1}	Water free 100 s^{-1}	50% emul. 10s^{-1}	75% emul. 10s^{-1}
Wisting Central	250 °C+	150 l	0.887	< −36	0.08	1.2	199	192	2538	5869
Troll B	250 °C+	250 l	0.923	−9	0.04	0.9	923	873	6278	11,299
Grane	200 °C+	330 l	0.952	−18	3.9	3.3	5981	5445	15,945	
	270 °C+	170 l	0.965	N/A	4.2	3.6	33,927	26,248	273,691	
Oseberg Blend	200 °C+	60 l	0.883	12	0.29	3.9	882^{A}		8682	
	250 °C+	150 l	0.905	18	0.35	4.6	1090^{A}		22,612	
Marine Gas Oil	Fresh	1 barrel	0.851	< −36	0.02	0.81	8		N/A	

A: Measured at 13 °C. Shear rates for viscosity measurements: 10 and/or 100 s^{-1}.

Table 2
Methods and instrumentation for analysis of physicochemical properties.

Property	Analytical method	Instrumentation
Evaporative loss	GC/FID	Agilent 6890N. 30 m DB1 column
Density	ASTM method D4052-81	Anton Paar DMA 4500
Pour point	ASTM method D97	
Asphaltene content	IP 143/90	
Wax content	Bridié et al., 1980	
Viscosity	McDonagh et al., 1995	Physica MCR 300

Table 3
Series of experiments performed in the two ice scenarios studied.

Scenario		Description
Solid ice:	1a	Oil thickness against a solid ice barrier
	1b	Horizontal movement of oil droplets under the ice sheet
	1c	Droplet formation in front of a solid ice barrier
Frazil ice:	2a	Horizontal migration of oil in frazil ice
	2b	Vertical migration of oil droplets in frazil ice
	2c	Vertical migration of oil in frazil ice
	2d	Droplet formation in frazil ice

Table 3) and horizontal and vertical movement of oil under or in ice (1b, 2a, b and c). Droplet formation, after exposure to breaking waves, in front of solid ice and in frazil ice (1c and 2d) is not addressed in this paper but will likely be presented in an upcoming paper.

4.1. Oil thickness against a solid ice barrier

A series of 12 experiments with five different oil samples at different degrees of weathering were performed (see Table 4). In each experiment three different oil volumes were tested, starting with 2.5 l. Then an additional 2.5 l were added to give a total of 5 l and finally 5 l were added for a total of 10 l in the flume. For each volume increment, the extent and thickness of the oil film in front of the “ice” barrier were measured at five to six different current settings (5, 10, 15, 20 25 and 30 cm/s).

4.2. Horizontal movement of oil droplets under a solid ice sheet

Øksenvåg et al. (2019) studied potential adhesion of oil to sea ice using a simple dipping test combined with more sophisticated measurements of surface tension and contact angle and found that it was negligible when the ice was wetted by water. The aim with this limited number of experiments was to verify these findings and to study the movement of oil droplets under ice and the water current velocities needed to move the oil droplets under varying under-ice roughness. The results were compared to similar experiments done by Buist et al. (2008). Three different under-ice structures, with different roughness, were used in this testing (Fig. 4). The solid ice sheet prepared from low salinity water, as described above, represent a very hard and smooth underside (Fig. 4A). It is more representative for freshwater ice than seawater ice but was a good candidate to test potential adhesion of oil droplets. According to Buist et al. (2008) it represents low under-ice roughness (factor: 1). A 2–3 cm layer of frazil ice was made from sea water in the flume overnight by gentle wave movements in the water surface. The solid ice sheet was carefully placed on top of this layer of frazil ice, pushing it 10 cm into the water (Fig. 4B). This represented a rougher saline ice layer given an under-ice roughness factor of 2 (Buist et al., 2008). The third under-ice structure was a 4–6 cm thick skeletal ice layer prepared from sea water in the flume over three days without any wave movements in the surface. This is assumed to be representative for natural sea ice providing a high under-ice roughness factor (Fig. 4C).

In total, five experiments with five different weathered oils were performed. Droplets were continuously released from a syringe under the ice at given time intervals. Photos were taken at a given rate (1 image per second), using the SLR camera (Fig. 3), in order to study the movement of the oil droplets as a function of current velocity. Waves were not used in these experiments. Current velocities of 5, 7, 10, 12, 20, 25 and 30 cm/s were used. Images were processed to provide drift speed and droplet size. Droplets were tracked using the Trackpy package in the Python programming language (Python Software).

Table 4
Weathered oil samples used in testing of oil thickness against a solid ice barrier.

Oil	Residue	Water free	50% emulsion	75% emulsion
Wisting C	250 °C	X	X	X
Troll B	250 °C	X	X	X
Grane	200 °C	X	X	
	270 °C	X		
Oseberg Blend	200 °C		X	
	250 °C		X	
Marine Gas Oil	Fresh	X		

4.3. Horizontal and vertical movement of oil in frazil ice

Horizontal movement on top of a frazil ice layer and vertical rise velocities of weathered oil/emulsion through a layer of frazil ice was extensively studied. Frazil ice was prepared in the flume as described in Section 3.3. The amount of ice was adapted so that a 10 cm thick layer of ice, covering the area from the back of the flume to approximately the mid-point, could be maintained at a current speed of 10 cm/s (see Fig. 2). It was possible to perform several experiments without changing the ice or making additional ice as the most oil contaminated ice was easily removed using a strainer.

Experiments were performed with six weathered oil samples (X in Table 5) to study the potential for horizontal migration of weathered oil in frazil ice. An oil sample of 500 ml was carefully applied on top of the frazil ice at the leading edge of the ice field. The experiments typically started with a wave setting of 3 cm amplitude (wave height of 6 cm) and a frequency of 1.5 Hz (in open water). The current speed was 10 cm/s during all experiments. When the movement of the oil in the ice stopped or became significantly lower relative to the frazil ice, the frequency was decreased to 1.25 Hz leading to further movement of oil inside the ice field.

It is expected that oil can appear as droplets under ice. Mechanisms contributing to formation of oil droplets drifting under ice can be:

- When oil confined against sea ice or drifting in the vicinity of the ice is exposed to breaking waves, oil droplets may be formed and transported under the ice by currents (referred to as natural dispersion).
- Dispersants can be used to create small oil droplets in the water column (referred to as chemical dispersion). The oil droplets are typically smaller than those formed by natural dispersion and have less buoyancy but can still resurface under ice.
- Subsea releases may also contribute to formation of oil droplets that rise under the ice.

A total of five experiments with droplets from weathered oil samples (Y in Table 5) were performed to study the vertical rise velocities through a layer of frazil ice. In these experiments the oil was applied as discrete droplets under the ice by use of a syringe. The droplet size varied with the viscosity of the oil. Grane 200 °C+ and Troll B

Fig. 4. Pictures of the ice structures used in testing of horizontal movement of oil droplets under ice. A: Smooth ice; B: frazil ice; C; skeletal ice layer.

Table 5
Weathered oil samples used in testing of horizontal and vertical movement of oil in frazil ice.

Oil	Residue	Water free	50% emulsion
Wisting C	250 °C	XYZ	XZ
Troll B	250 °C	YZ	YZ
Grane	200 °C	YZ	XZ
	270 °C	X	
Oseberg Blend	200 °C		Z
	250 °C		X
Marine Gas Oil	Fresh	XYZ	

X: Horizontal migration of 500 ml weathered oil batches.
Y: vertical migration of weathered oil droplets.
Z: vertical migration of 60 ml weathered oil batches.

250 °C+/50%, both with a viscosity around 6000 cP produced droplets with a diameter of around 10 mm. The other oil samples, having lower viscosity, resulted in smaller oil droplets. The wave generator was adjusted to produce a wave with an amplitude of 3 cm (wave height of 6 cm) and a frequency of 1.25 Hz in open water. The oil droplets were applied approximately 1 m inside from the leading edge of the ice field (position B in Fig. 2). The effective wave amplitude in this position was 2 cm and the ice thickness approximately 9 cm. The current speed was set to 5 cm/s. The vertical rise was recorded after 30 s periods, then every minute until 10 min had lapsed.

Larger volumes (60 ml) of water-free oils/emulsions were applied under the ice using a syringe. Eight weathered oil samples (Z in Table 5) were tested at two different release points in the ice for a total of 16 experiments performed. With reference to Fig. 2, release point B was approximately 1 m and release point A approximately 2 m inside from the leading edge of the ice field. The current speed was 5 cm/s, the wave amplitude (in open water) was 3 cm and the wave frequency (in open water) was 1.25 Hz. The wave amplitude measured in the ice was 2 cm at release point B and 1 cm at release point A. Therefore, the overall energy input was higher at point B than point A.

5. Results and discussion

5.1. Oil thickness against a solid ice barrier

The main objective of these experiments was to support modelling of oil thickness in the presence of an ice edge. In open water and low ice coverage the transport of oil on the surface is being controlled mainly by wind and current, but is more controlled by the ice if it is trapped in high ice coverage (Venkatesh et al., 1990; French-McCay et al., 2018; Nordam et al., 2019). Oil spilled close to sea ice may be transported into the ice by wind and currents and may be concentrated to higher

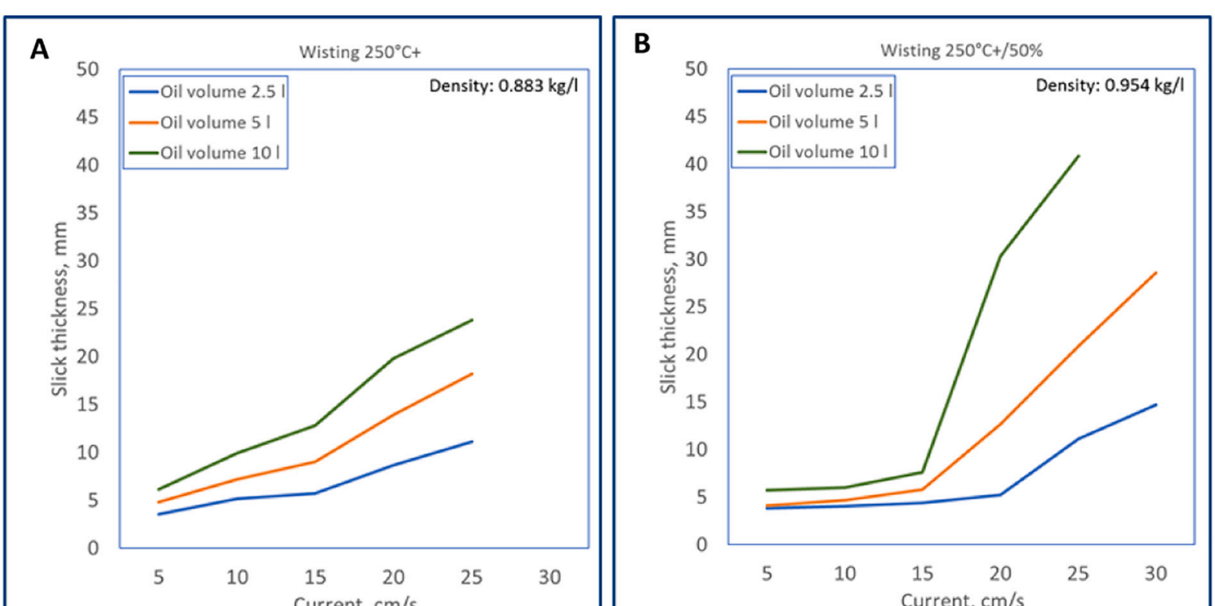

Fig. 5. Slick thickness against a solid ice barrier as a function of water current and oil volume for Wisting Central crude. Evaporated oil in A and emulsified oil in B.

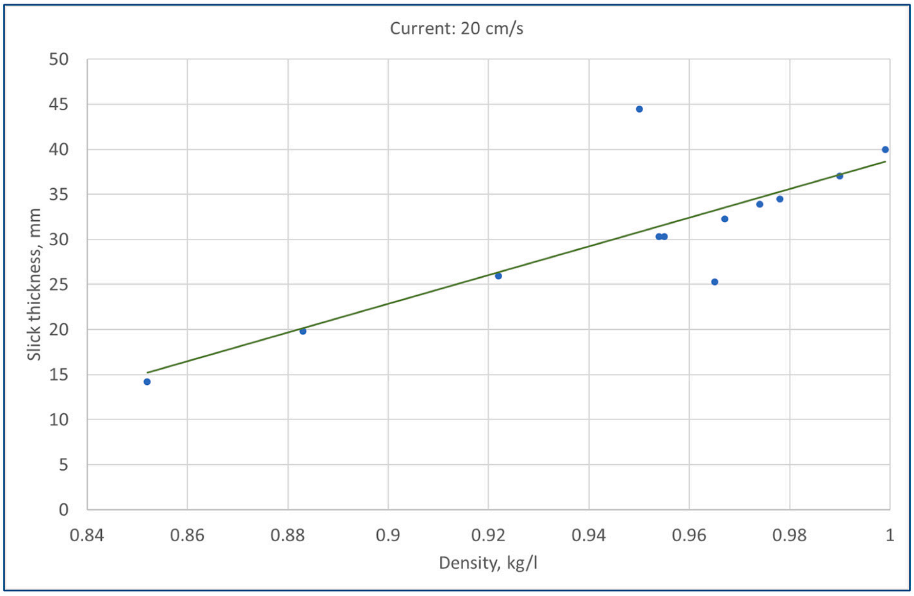

Fig. 6. Slick thickness as a function of density including a linear trendline, based on data when using 10 l of weathered oil and a current of 20 cm/s.

thicknesses. This may resemble the collection of oil in a boom during oil spill response operations.

In this testing oil volume was systematically increased in each experiment (2.5–5–10 l) as described in Section 4.1. As expected, the oil thickness against the solid ice barrier increased with increasing oil volume. Fig. 5 shows an example of measurements taken during experiments with Wisting Central crude oil: an evaporated but non-emulsified oil sample in Fig. 5A and an emulsion sample in Fig. 5B. The general observation was that oil slicks compressed against the ice barrier with increasing current velocity, resulting in an increase in slick thickness. However, for some of the more viscous oils, the compression was small at the lower current settings (typically 15 cm/s and less) but increased considerably when current velocities exceeded 15–20 cm/s.

The current theory describing oil confined against a barrier or in an oil boom suggests that the thickness of the oil is determined by the balance of two forces: the pressure force, due to the difference in density between oil and water, and the friction force between water and oil, due to the current. Results from these experiments have been used to compare and verify the current theory used to model oil thickness in the presence of an ice barrier and is discussed by Nordam et al. (2020).

Fig. 6 presents a plot of density versus slick thickness for the twelve oil samples defined in Table 4, at a current velocity of 20 cm/s for an oil volume of 10 l. Results indicate a trend of increasing thickness with increasing density. The light (low-density) MGO produced the smallest slick thickness, while the Troll B 250 °C+/50% emulsion, with a density close to 1, produced the greatest thickness. There are two outliers in this plot: Grane 200 °C+ with a density of 0.950 kg/l and Oseberg Blend 250 °C+/50% emulsion with a density of 0.965.

The theory, based on density of the oils as an input, assumes Newtonian behaviour for the oils. Most of the weathered oil samples tested in this project exhibited more or less non-Newtonian behaviour. It was observed that for weathered oils other physicochemical parameters, such as viscosity and pour point, also play a role in slick behaviour and oil thickness.

In the experiments performed three different kind of behaviour were observed. This is illustrated through pictures in Fig. 7. Some of the lighter and low-viscous water-free oils (Marine Gas Oil (MGO), Wisting C 250 °C+ and Troll B 250 °C+ residues) formed a relatively even thickness distribution when contained against the ice barrier and were less influenced by current speed than the more viscous weathered oils. This is illustrated in pictures A and B represented by MGO. The Oseberg Blend emulsion (picture C and D), with high pour point, tended to solidify in contact with the cold sea water, forming a rigid, discontinuous layer of oil with free water between the oil lumps. This layer was not easily compressed by currents. The medium- to high-viscosity emulsions (evaporated Grane samples and emulsions from most test oils) formed “lips” of thicker oil in the front end of the slick when pushed against the ice barrier. When exposed to strong current (25–30 cm/s), the leading edge of the oil slick became increasingly thick at the ice barrier and combined with high density the oil was pushed under the ice.

5.2. Horizontal movement of oil droplets under a solid ice sheet

The objective of these experiments was to confirm that movement of oil droplets under ice is a function of under-ice roughness and current velocity and that adhesion of oil to ice is minor or negligible. The study was limited to three weathered oil samples (Wisting C 250 °C+ residue, Wisting C 250 °C+/50% emulsion and Grane 200 °C+/50% emulsion) and MGO, tested in three different ice structures with different roughness (see Section 4.2). Oil droplets were continuously released under the ice and the movement of the individual droplets along the underside of the ice sheet was recorded using a camera as described in Section 3.1. Fig. 8 gives an example of tracking of oil droplets from the experiment with Wisting C 250 °C+. Fig. 8A shows the trajectories of all the droplets monitored within the camera frame. The droplets were applied to the right of the frame. Fig. 8B gives a distribution of drift velocities for all droplets. Mean drift velocity was approximately 2 cm/s.

Adhesion of oil to solid sea ice is minor or negligible, provided that the ice is wetted by sea water (Øksenvåg et al., 2019). The horizontal movement of oil under ice may therefore be expected to follow the direction of the water mass (current) and the velocity will be dependent on the under-ice roughness hindering the drift of the oil droplets. In these experiments, clear differences in oil droplet velocity were observed between the different under-ice structures whereas the oil types, properties and degree of weathering seemed to have little effect. However, this observation is based on a limited set of data and should be regarded as a trend rather than an unambiguous conclusion.

Fig. 9 sums up all the horizontal velocity measurements recorded in this test series, where drift velocity was measured as a function of increasing current. In the experiments with smooth ice the three oil samples tested produced oil droplets with different size. Grane

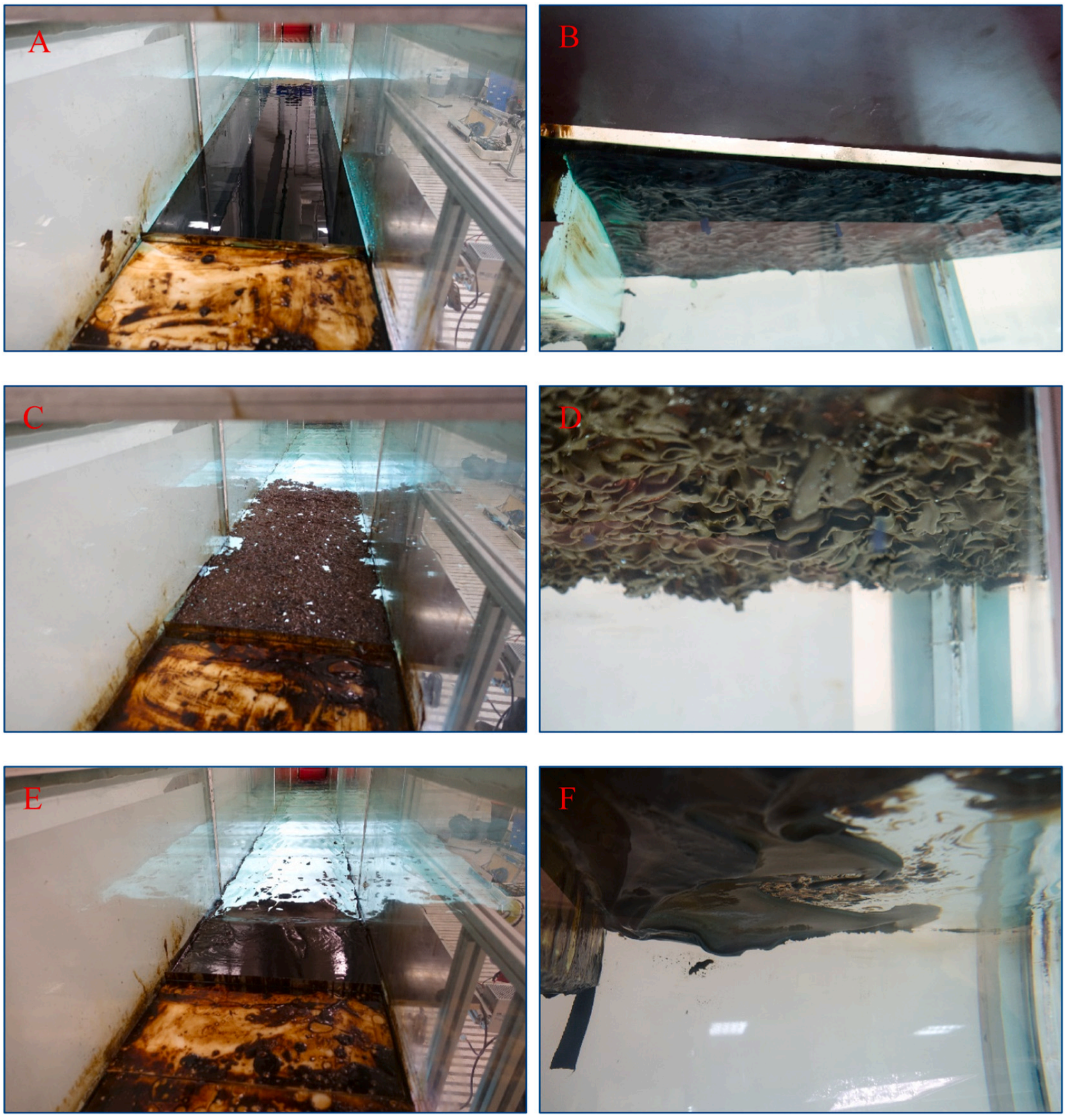

Fig. 7. Pictures from selected experiments showing:
A: Marine Gas Oil (MGO). Surface image at 5 cm/s current with 10 l oil.
B: Marine Gas Oil (MGO). Sub-surface image at 15 cm/s current with 5 l oil.
C: Oseberg Blend 250 °C+/50%. Surface image at 5 cm/s current with 10 l oil.
D: Oseberg Blend 250 °C+/50%. Sub-surface image at 20 cm/s current with 2.5 l oil.
E: Grane 200 °C+/50%. Surface image at 5 cm/s current with 10 l oil.
F: Grane 200 °C+/50%. Sub-surface image at 25 cm/s current with 2.5 l oil.

200 °C+/50% emulsion produced slightly larger oil droplets than the Wisting C 250 °C+/50% emulsion which in turn produced larger oil droplets than MGO. There was no clear indication that different droplet sizes affected the drift velocity within the size range tested in these experiments (< 12 mm). The grey trend line in Fig. 9 represent the maximum drift velocity for droplets in the smooth ice experiments. Movement was observed starting at a low current speed (5 cm/s). Drift velocity increased with increasing current speed. Observations were carried out until most droplets had moved out of the camera frame (> 25 cm/s). The red dot represents the median drift velocity at 12 cm/s current for Wisting C 250 °C+ as presented in Fig. 8. For the frazil seawater ice surface experiments (blue line) the droplets started to move slightly after 20 cm/s and the first measured drift velocity was registered at 25 cm/s. The same behaviour was observed in the skeletal ice surface experiment (yellow line), but at a lower drift velocity.

Re-calculation of the drift velocity readings from the trendlines in Fig. 9 at the different current speeds used, results in the following "mean" drift velocity as a percentage of current speed:

Ice	Current Speed (CS), cm/sec	Drift Velocity (DV), cm/sec	DV in % of CS
Smooth	5	0.1	2
	7	0.2	3
	10	1.2	12
	12	2.2	18
	20	2.4	12
Frazil	25	1.6	6.4
	30	1.7	6.0
Skeletal	25	0.61	2.4
	30	0.60	2.0

For the smooth ice block, the highest value was observed at a current velocity of 12 cm/s resulting in a mean oil droplet drift velocity of 18% of the current speed. For the frazil ice this percentage dropped to

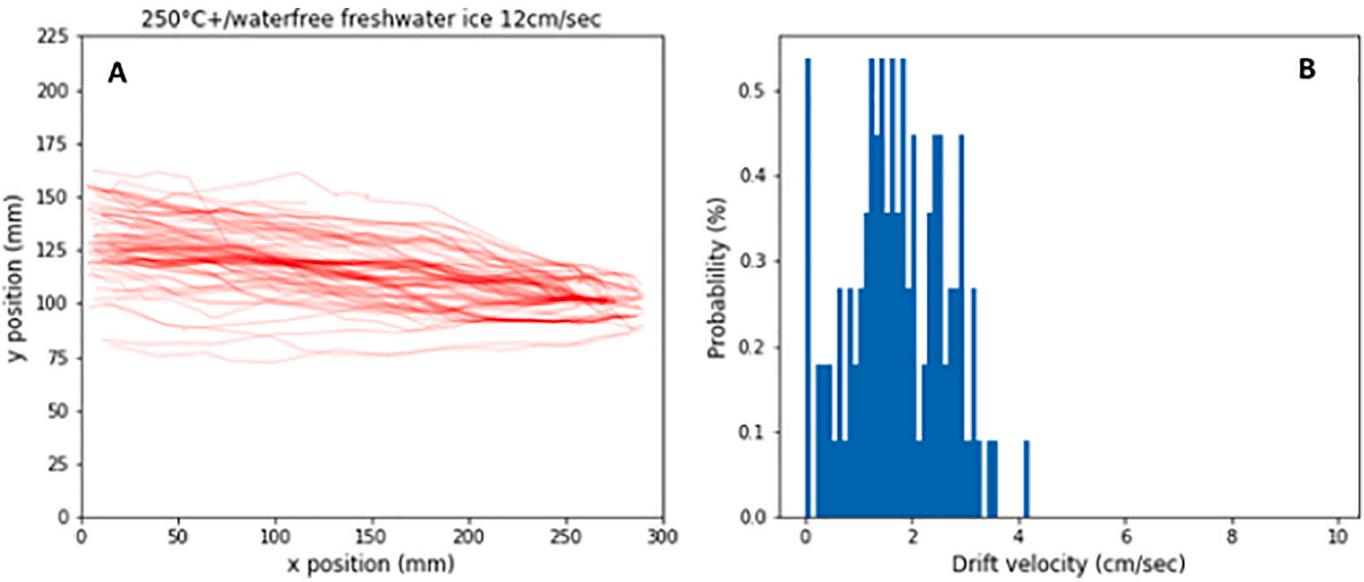

Fig. 8. Example of tracking of the oil droplets from the experiment with Wisting C 250 °C+. A: Trajectories of a large number of droplets within the frame covered by the camera (300 × 225 mm). Droplets were applied to the right of the frame. B: Distribution of drift velocities in cm/s.

around 6% and for the skeletal ice it was around 2%. From this limited number of experiments, it has been demonstrated that the ice conditions and the "structure" under the ice sheet plays a very important role in the movement of oil droplets under ice.

Buist et al. (2008) did some experiments studying oil movement under ice in a wind/wave tank. The aim was to quantify the minimum water velocities (stripping velocity) required to start moving crude oil droplets under sea ice with focus on the effect of oil properties, under-ice roughness and salinity of the ice. An under-ice roughness factor was used to calculate stripping velocity from the following equation by Cox and Schultz (1980):

$$Uth = Ci\left(\frac{305.79}{88.68 - \mu o}\right)$$

where: Uth = Threshold stripping velocity (cm/s); μo = oil viscosity in Poise; Ci = under-ice roughness factor, which varies from 1 for smooth freshwater ice through 2 for saline ice to 6 for any refrozen rubble ice. Using this equation combined with the results from the tank experiments performed, stripping velocities of 3–5 cm/s were found for smooth freshwater ice, 7–10 cm/s for smooth saline ice and up to 15–20 cm/s for undulating saline ice. Only current (no wave movements) was used in our experiments, but there is a relatively good correlation between the results reported by Buist et al., and the results from the experiment performed in this project.

It is important to recognize that the underside of a sea ice layer at sea normally will be more rugged and cracked than simulated in these experiments. In conditions where ice floes of different sizes are pushed together, there will be spacing between the floes where oil and oil droplets may rise to the surface and become trapped. The roughness

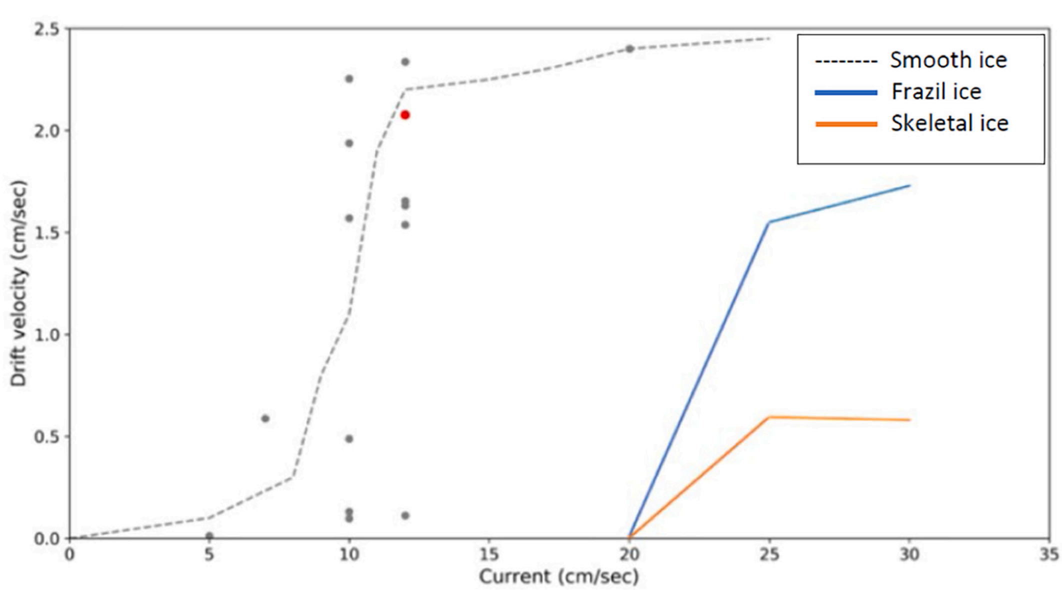

Fig. 9. Horizontal drift velocity measured for Wisting C weathered water-free residues and emulsions as a function of current in the flume for three different ice conditions: smooth freshwater ice (grey and red dots + trendline), frazil seawater ice (blue line) and skeletal ice (yellow line). (For interpretation of the references to colour in this figure legend, the reader is referred to the web version of this article.)

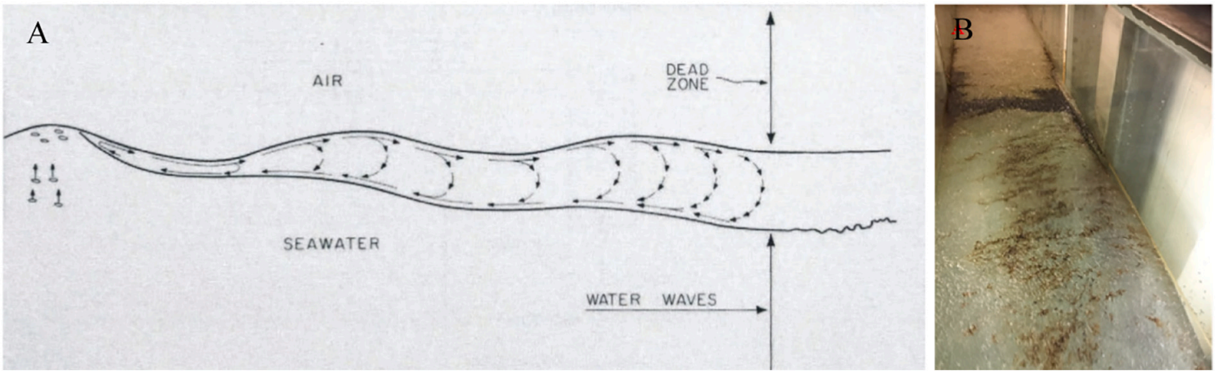

Fig. 10. Drawing illustrating the main circulation in grease ice. Illustration by Martin and Kauffman (1981) (A) and a picture from testing with Wisting C 250 °C+ in frazil ice in the wave and current flume (B).

and characteristics of the ice will have a greater effect on the horizontal movement of oil under solid ice than oil properties because adhesion of oil to ice wetted by seawater is minor.

5.3. Horizontal and vertical movement of oil in frazil ice

Areas with frazil ice have often been observed in the Norwegian Barents Sea, especially in late winter or early springtime (see Fig. 1). It has also been observed that waves formed in the open sea can propagate into the ice field. The interaction of weathered oil in ice under such conditions is not well documented. A study from 2008 on "Waves in Sea Ice" (Brostrøm and Christensen, 2008) provides an overview on how waves and ice interact in the ocean and describes the most relevant ice characteristics found in the ocean. Wave-ice interaction is challenging to describe in detail, and advanced mathematical models are often used to describe it. Their study suggests that waves occurring in the interior area of the Marginal Ice Zone (MIZ), closest to the solid pack ice, have very week amplitude and long wavelength. Amplitude decreases as the wave energy travel through the increasingly dense ice coverage and energy is scattered. Shorter waves (high frequency) are scattered more efficiently than longer waves (low frequency) implying that only the low frequency waves can penetrate deep into the MIZ.

Martin and Kauffman (1981) studied wave propagation in and wave damping by grease ice. Based on experiments in a wave tank, a drawing of the main circulation in the grease ice was prepared (Fig. 10A). To the left-hand side of the figure, individual ice crystals rising to the surface is illustrated. Once they reach the surface, they are swept into the grease ice by Stokes drift. The grease ice is then herded to the right into a long oscillatory wedge. The arrows within the liquid grease ice show the direction and approximate magnitude of the mean circulation. The diagram also shows a vertical line marked as the "dead zone". This represent the area where the waves are decayed, and the grease ice changes from a "liquid" to "solid" behaviour. This means that to the left of the "dead zone" the waves propagate as water waves with strong relative motions within the ice. To the right of the "dead zone" the ice appears to move as an elastic solid with no internal relative motion. In general, the "dead zone" serves both as a transition between liquid and solid behaviour and as an "accumulation line" for material released on the surface.

Experiments with six weathered oil/emulsion samples were performed to study the potential for horizontal migration of weathered oil in frazil ice. The weathered oil samples were applied at the leading edge of the ice field. Fig. 10B shows a picture from a test with Wisting C 250 °C+. For all oils tested (Fig. 11) the migration slowed down or stopped when the oil reached the "dead zone" but continued to migrate when the wave frequency was reduced (from 1.5 Hz to 1.25 Hz). This is in accordance with the theory described above. Two evaporated but water free oil residues, Wisting C 250 °C+ and Grane 270 °C+ were tested (Fig. 11A and B) and showed different behaviour under similar test conditions. Initially, the Grane 270 °C+ oil floated out onto the ice surface. Once it had cooled to sea ice temperature, it started to form small lumps that were transported downwards to the underside of the frazil ice, then started to move backward towards the leading edge of the ice field. At that point, the lumps encountered the surface again and started to move forward on top of the ice. The same circular phenomenon was also observed with Oseberg Blend emulsion (Fig. 11D). The movement of oil lumps to the underside of the ice layer is assumed to be a result of the high viscosity combined with the high density, while the movement forward on top of the ice and backwards under the ice can be explained Stokes drift as described by the observations of Martin and Kauffman (1981) (Fig. 10). Wisting C 250 °C+ has much lower viscosity and density than Grane 270 °C+ which explains the difference in behaviour between these two oils.

The test series carried out to study the horizontal migration in frazil ice were performed on a selection of weathered oils that covers a wide spectrum of physicochemical and emulsion properties. Observations showed that for oil to move horizontally inside an ice field with frazil ice, wave movement is required. As long as there was wave movement, the oil moved forward on the ice surface, while oil that moved to the underside of the ice was drawn backwards by the wave movement. A current shear between the sea water and the ice was not sufficient to initiate movement of weathered oil into the ice field. When the wave action levelled out at the "dead zone", the forward movement of the oil stopped as there was no internal relative movement in the ice. It has been demonstrated that decreasing the wave frequency can cause the weathered oil to travel further into the frazil ice. Wave frequency was more important than amplitude in causing the oil to move in a frazil ice field.

It was observed that the heavier and highly viscous oils could form lumps with a potential to move through the ice to the underside where it was transported in the opposite direction. This formation into lumps and movement through the ice can be explained by a combination of high viscosity, high density, and/or high pour point (for the Oseberg Blend emulsion). Therefore, oil type, weathering degree and physicochemical properties seem relevant to the horizontal migration of oil in frazil sea ice.

The vertical movement in frazil ice was further studied by applying both oil droplets and 60 ml batches of oil under frazil ice and expose it to wave activity. In this series of experiments, 8 evaporated and/or emulsified oil samples, including the fresh MGO, were tested. Fig. 12 shows photos from tests with 60 ml batch tests of Oseberg Blend 200 °C+/50% and MGO. A clear difference in appearance was observed, with the heavy Oseberg Blend emulsion forming larger lumps that was imbedded at the underside of the ice layer and the lighter Marine Gas Oil (MGO) forming smaller lumps (typically 1–10 mm in diameter).

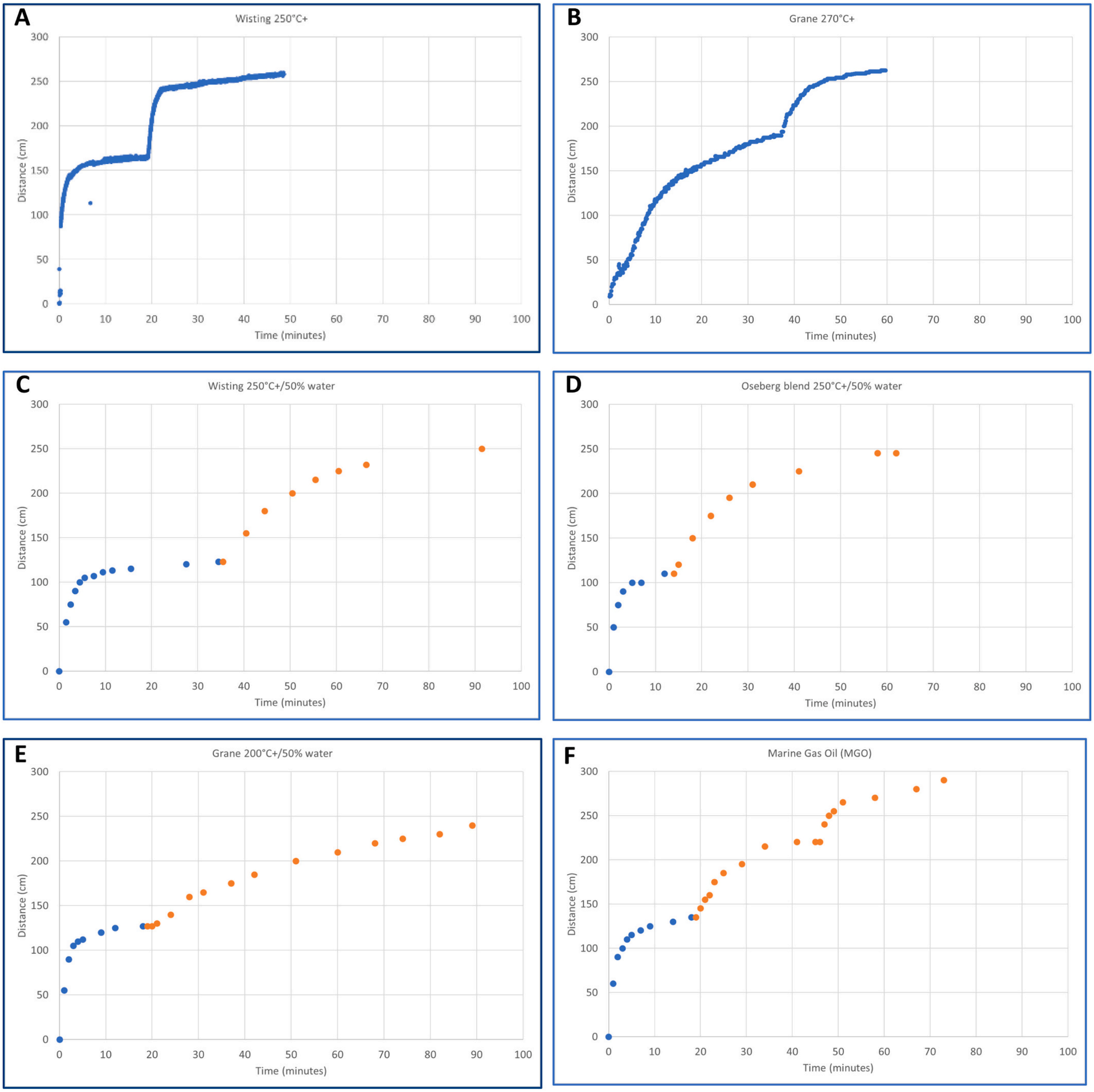

Fig. 11. Distance of horizontal migration in frazil ice. 10 cm/s current. Initial Wave: Frequency 1.5 Hz; Amplitude 3 cm.
A: Wisting C 250 °C+. Wave frequency: 1.25 Hz after 19 min (min).
B: Grane 270 °C+. Wave frequency: 1.25 Hz after 38 min.
C: Wisting C 250 °C+/50% emulsion. Wave frequency: 1.25 Hz after 36 min.
D: Oseberg Blend 250 °C+/50% emulsion. Wave frequency: 1.25 Hz after 14 min.
E: Grane 200 °C+/50% emulsion. Wave frequency: 1.25 Hz after 19 min.
F: Marine Gas Oil (MGO). Wave frequency: 1.25 Hz after 19 min. Amplitude from 3 to 4 cm after 46 min.

Fig. 13 shows the results from the vertical migration test series in the position in the ice with lowest energy (position A), using 60 ml batch releases of weathered oil. The position of the upper part of the migrating oil, visualized as the vertical position in the 10 cm thick ice layer, is plotted as a function of time after application of the oil sample under the ice layer. MGO migrated quickly to the ice surface while the heavier weathered oils migrated more slowly or did not reach the surface within the 10 minute test period and showed a tendency to remain imbedded in the frazil ice.

There was a clear trend observed between viscosity of the weathered oils and the vertical migration distance and speed. The highest viscosity oil tested (Grane 200 °C+/50% emulsion; viscosity approximately 16.000 cP) resulted in the shortest migration distance, while for instance Wisting C 250 °C+, with a viscosity of 200 cP, reached the surface after 2 min. The same trend was to some degree also observed as a function of the density of the weathered oils. Similar experiments

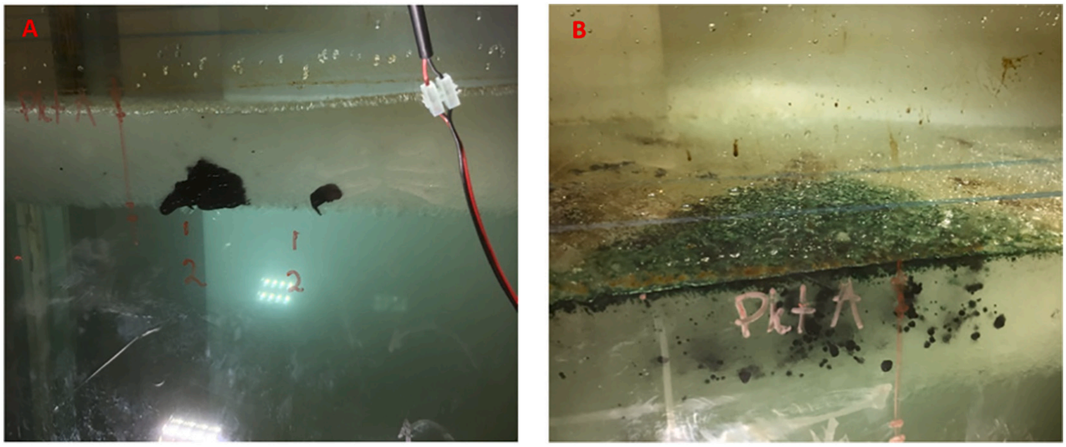

Fig. 12. Examples from testing of vertical migration of oil in frazil ice using 60 ml batches applied under the ice. A: Oseberg Blend 200 °C+/50% emulsion. B: Marine Gas Oil (MGO).

were carried out with the same weathered oils at a slightly higher wave energy (position B in Fig. 2). The wave and current settings were the same in both series of experiments. However, in the ice a wave amplitude of 1 cm was measured in position A and a wave amplitude of 2 cm was measured in position B, 1 m from the leading edge of the ice field. Due to the higher energy input (wave amplitude), the vertical migration speed was higher in position B for all oils. Three of the weathered oils still did not reach the surface within the 10 min testing period and remained imbedded in the ice layer.

Testing with application of oil droplets under the ice, indicated a different migration pattern. While the 250 °C+ residues of Wisting C and Troll B reached the surface after 2 min in the 60 ml batch release, they did not reach the surface during the 10 min testing period when released as droplets. Troll B 250 °C+/50% emulsion did not show any vertical migration in the droplet experiments but migrated upwards in the 60 ml experiments in both positions (A and B). Sampling and analysis of the frazil ice revealed that it contained approximately 60% free water with a salinity of 3.5% and a density of 1.024 kg/l. After the free water was drained off and the remaining ice was melted, the density of the melting water was close to that of fresh water (approximately 0.917 kg/l) so the frazil ice had a high buoyancy in sea water. There might be a gradient in the “grained” frazil ice where the crystals are packed denser in the upper part of the ice layer. This might explain why some of the weathered oils did not rise to the surface: high viscosity prevented the migration of oil between the densely packed grained ice particles and the density of the ice (close to 0.92 kg/l) was lower than many of the weathered oils tested. The oil droplets moved horizontally under the ice layer to a greater extent than the 60 ml batches, which could explain why the vertical migration was lower.

Several studies have been performed on migration of oil in sea ice (e.g. Wilkinson et al., 2007; Karlsson et al., 2011; Petrich et al., 2013). A common basis for many earlier studies on oil migration in sea ice is migration through brine channels. This means that the ice was more solid and not frazil as in these experiments. The results from this study

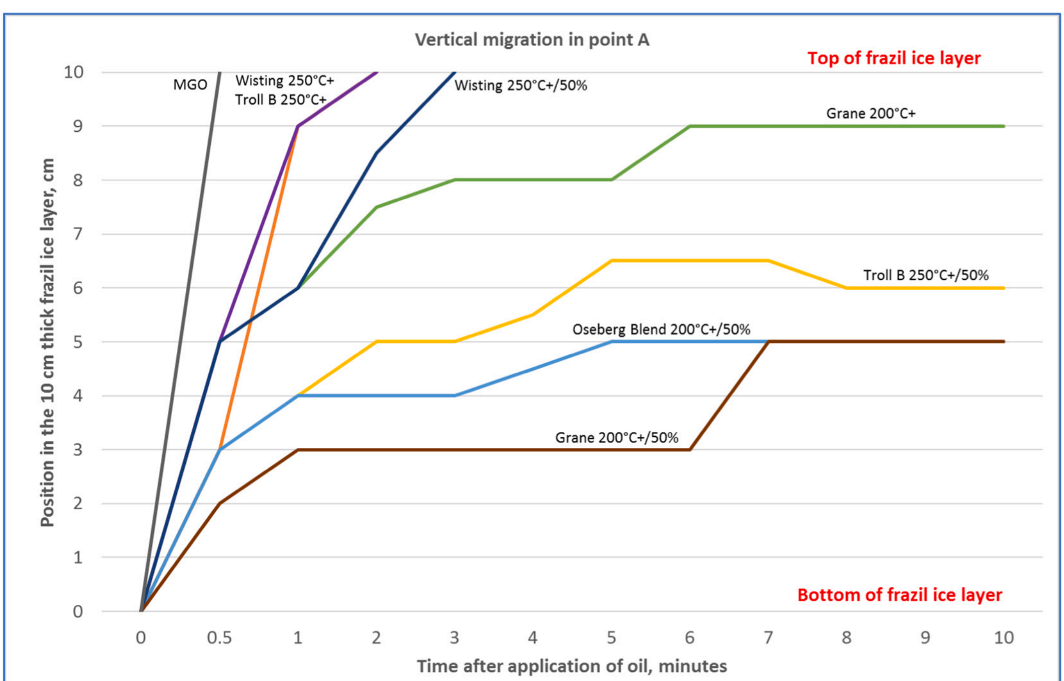

Fig. 13. Vertical migration in frazil ice in position A in Fig. 2 (lowest energy). Ice thickness was 10 cm and wave amplitude was 1 cm. Plotted as the vertical position in the ice layer (10 cm represents the ice surface) as a function of time after application of oil under the ice sheet.

indicate that there is a potential for weathered oil to migrate both vertically and horizontally in frazil ice provided there is sufficient wave energy. Many weathered oils, if pushed under ice, are likely to migrate towards the surface of a frazil ice layer, while in a solid sea ice scenario they will tend to stay under the ice or be encapsulated in the ice. Wilkinson et al. (2014) studied the behaviour of a fresh crude oil under three different ice types: frazil ice, nilas and pancake ice. In the frazil ice experiment the oil did not spread laterally across the bottom of the ice, as with the other ice types, but penetrated the frazil layer until it reached the uppermost frazil layer at the seawater surface. This was a fresh crude oil with lower viscosity and density than most of the weathered crude oils used in this study. However, it might be compared to the Marin Gas Oil and confirm findings from this study.

Trites et al., 1986 modelled movement of Bunker C after a spill from the tanker "Kurdistan" into the waters and ice of the Cabot Strait, Nova Scotia. They observed that some of the drifting oil contacted ice and became incorporated and trapped within the ice field. The oil was carried with the ice. Accidental oil spills where the oil encounters ice is rare, but the findings from Trites confirm what we have seen in this study that oil can migrate into an ice field and be incorporated in the ice.

6. Conclusions and recommendations

Two different ice regimes (solid and frazil ice) were simulated in a novel current and wave flume to study the interaction between weathered oil and ice. Seven series of experiments were defined under these two ice regimes. The oils, selected for this project, represented a broad range of physicochemical properties. Prior to testing, the oils were evaporated in a large-scale topping tank, and emulsions were prepared from the evaporated residues to simulate weathered oil that has drifted for some time on the sea surface (typically 1–3 days) before encountering sea ice. Test oils included both evaporated water-free oils and emulsions. Solid ice was prepared from low salinity (0.5%) water in a freezing room while frazil ice was produced from sea water in the flume, at ambient temperatures of −4 to −5 °C over a period of 1–2 days.

6.1. Ice regime: solid ice barrier

Experiments conducted to study the thickness of different weathered oils drifting against a solid ice barrier indicated that there is a distinct difference between different weathered oils. It has been demonstrated that increased density of the weathered oil gives increased thickness, but viscosity and pour point also contributed to the oil's behaviour at the ice barrier. Some of the lighter, low-viscous, and water-free oils formed a relatively even thickness distribution and were also less influenced by current speed than the more viscous oils/emulsions. Weathered oils with high pour point tended to solidify in contact with cold sea water and formed a solid oil layer with a lot of free water in between the oil lumps, which was not readily compressed by currents. Medium- to high-viscous emulsions formed "lips" of thicker oil at the leading edge of the slick when contained against a solid ice barrier. In strong currents, these oils have the potential to form a very thick layer at the ice edge and, in the case of oils with high density, be pushed under the ice. Results from these experiments have been used for comparison with a theory used to model oil thickness in the presence of an ice barrier (Nordam et al., 2020).

The second series of experiments in this ice regime demonstrated that the horizontal drift of droplets from weathered oil released under a solid ice layer is a function of the under-ice roughness. Adhesion of oil to solid sea ice is minor or negligible and the roughness of the underside of the ice layer influenced the friction between oil and ice and therefore the velocity of the oil moving under ice. Oil type, properties and degree of weathering seemed to have less significance on the drift velocity.

6.2. Ice regime: frazil ice barrier

It has been demonstrated that weathered oils can migrate horizontally on top of or vertically through an ice field composed of frazil sea ice. A current shear between the seawater and ice alone did not seem to be sufficient to induce horizontal movement of oil through the ice. Waves propagating through the ice field were needed for the oil to moved forward on the ice surface. If wave action was maintained, oil continued to move in a forward direction. As the wave action in the ice decreased, the forward movement of the oil eventually stopped. Open water waves with low frequency (long wavelength) can penetrate more deeply into ice than high frequency waves (short wavelength). It was observed that the weathered oil that formed lumps when spilled in cold sea water had the potential to move through the ice to the underside where it was transported in the opposite direction by wave actions in the frazil ice. High viscosity, high density and/or high pour point seem to be important for formation of lumps and their behaviour in frazil ice.

Testing of vertical movement of oil in frazil ice revealed large differences between the more heavy and high-viscous emulsions and the lighter water-free oils and Marine Gas oil. The high-viscous emulsions had the longest rising time and some of the emulsions were embedded in the ice and did not reach the surface. As for horizontal movement, wave activity is a prerequisite also for vertical migration in frazil ice. These experiments demonstrated that oil type, the degree of weathering and the physicochemical properties of the oil have a significance for both horizontal and vertical migration of oil in frazil ice.

6.3. Recommendations

Further flume studies of interaction between weathered oils and frazil and scattered ice should be performed. Such studies should also include a broader spectrum of fuel oils. It would be beneficial to carrying out field experiments in larger scale in actual Arctic conditions, to further validate the findings from flume or basin studies. Field trials can contribute to the knowledge regarding the use of dispersants and ISB, validate models and refine decision making tools for response in ice.

CRediT authorship contribution statement

Ivar Singsaas: Conceptualization, Methodology, Validation, Formal analysis, Investigation, Writing - original draft. **Frode Leirvik**: Investigation, Formal analysis, Methodology, Resources. **Per S. Daling**: Conceptualization, Validation, Methodology. **Chantal Guénette**: Writing - original draft, Conceptualization, Validation. **Kristin Rist Sørheim**: Conceptualization, Validation, Supervision, Project administration.

Declaration of competing interest

The authors declare that they have no known competing financial interests or personal relationships that could have appeared to influence the work reported in this paper.

Acknowledgements

This study was based on results obtained from a competence and knowledge building project within the Research Council of Norway (RCN) PETROMAKS2 program: "Fate, behaviour and response to oil drifting into scattered ice and ice edge in the marginal ice zone (FateIce)". The project was funded by RCN (contract no.: 255385/E30) and the Norwegian branch of the following international oil companies: AkerBP, ConocoPhillips, Eni Norge, Equinor, Lundin Norway, Neptune Energy, and OMV Norge. A reference group consisting of a representative from each of the following organisations: Norwegian Coastal Administration (NCA), Norwegian Clean Seas Association for

Operating Companies (NOFO), Eastern Canada Response Corporation Ltd (ECRC) has provided valuable scientific input to the project.

References

Beegle-Krause, C.J., Simmons, H., McPhee, M., Lundmark Daae, R., Reed, M., 2013. Literature review – fate of dispersed oil under ice. In: Arctic Response Technology Report 1.4.
Brandvik, P.J., Faksness, L.G., 2009. Weathering processes in Arctic oil spills: meso-scale experiments with different ice conditions. Cold Reg. Sci. Technol. 55, 160–166 2009.
Brandvik, P.J., Daling, P.S., Myrhaug, L.J., 2010. Mapping weathering properties as a function of ice conditions: a combined approach using a flume basin verified by large-scale field experiments. In: Proceedings of the Thirty-third AMOP Technical Seminar on Environment Contamination and Response. Environment Canada, Ottawa, Ontario, Canada, pp. 701–723.
Bridié, A.L., Wanders, T.H., Zegweld, W.V., den Heijde, H.B., 1980. Formation, prevention and breaking of seawater in crude oil emulsions, chocolate mousse. Marine Poll. Bull. 11, 343–348.
Brostrøm, G., Christensen, K., 2008. Waves in Sea Ice. (Met.no report no.: 5/2008).
Buist, I., Belore, R., Dickins, D., Guarino, A., Hackenberg, D., Wang, Z., 2008. Empirical Weathering Properties of Oil in Ice and Snow. Minerals Management Service, Alaska Environmental Studies Program, October 2008.
Cox, J.C., Schultz, L.A., 1980. The transport and behaviour of oil spilled under ice. In: Proceedings of the Third Arctic Marine Oilspill Program Technical Seminar. Environment Canada, Ottawa, ON, pp. 45–61 (1980).
Daling, P.S., Brandvik, P.J., Mackay, D., Johansen, Ø., 1990. Characterisation of crude oils for environmental purposes. Oil & Chemical Pollution 7, 199–224 1990.
Dickins, D., 2011. Behaviour of oil spills in ice and implications for Arctic spill response. In: Proceedings of the OTC Arctic Technology Conference, OTC 22126, 1–15. Houston, Texas, USA.
Dickins, D., 2017. Arctic Oil Spill Response Technology Joint Industry Programme. Synthesis Report. DF Dickins Associates, LLC.
French-McCay, D.P., Tajalli-Bakhsh, T., Jayko, K., Spaulding, M.L., Li, Z., 2018. Validation of oil spill transport and fate modeling in arctic ice. Arctic Science 4, 71–97.
Johansen, Ø., Brandvik, P.J., Farooq, U., 2013. Droplet breakup in subsea oil releases – part 2. Predictions of droplet size distribution with and without injection of chemical dispersants. Mar. Pollut. Bull. 73, 327–335.
Karlsson, J., Petrich, C., Eicken, H., 2011. Oil entrainment and migration in laboratory-grown saltwater ice. In: Port and Ocean Engineering under Arctic Conditions, July 10–14, 2011, Montreal Canada.
Martin, S., Kauffman, P., 1981. A field and laboratory study of wave damping by grease ice. J. Glaciol. 27 (96), 283–313 1981.
McDonagh, M., Hokstad, J.N., Nordvik, A.B., 1995. Standard procedure for viscosity measurement of water-in-oil emulsions. In: Marine Spill Response Corporation, Washington, D.C. MRSC Technical Report Series 95-030, (36 p).
Nordam, T., Beegle-Krause, C., Skancke, J., Nepstad, R., Reed, M., 2019. Improving oil spill trajectory modelling in the arctic. Mar. Pollut. Bull. 140, 65–74.
Nordam, T., Litzler, E., Skancke, J., Singsaas, I., Leirvik, F., Johansen, Ø., 2020. Modelling of oil thickness in the presence of an ice edge. Mar. Pollut. Bull. 156.
Øksenvåg, J.H.C., Fossen, M., Farooq, U., 2019. Study on how oil type and weathering of crude oils affect interaction with sea ice and polyethylene skimmer material. Marine Pollution Bulletin, Volume 145 (August 2019), 306–315.
Petrich, C., Karlsson, J., Eicken, H., 2013. Porosity of growing sea ice and potential for oil entrainment. Cold Reg. Sci. Technol. 87, 27–32.
Ramstad, S., Øksenvåg, J.H.C., Oltedal, T.A., Johansen, B., Leirvik, F., 2008. C2.2 - meso-scale weathering and characterisation of crude oils. In: Coastal Oil Spill JIP Report no 14 SINTEF Report No.: F9127.
Smedsrud, L.H., Skogseth, R., 2005. Field measurements of Arctic grease ice properties and processes. Cold Reg. Sci. Technol. 44 (3), 171–183 April 2006.
Sørstrøm, S.E., Brandvik, P.J., Buist, I., Daling, P.S., Dickins, D., Faksness, L.G., Potter, S., Fritt-Rasmussen, J., Singsaas, I., 2010. Joint industry program on oil spill contingency for Arctic and ice-covered waters. In: Summary Report SINTEF 2010, (ISBN 9788214047592).
Trites, R.W., Lawrence, D.J., Vandermeulen, J.H., 1986. Modelling oil movements from the Kurdistan spill in Cabot Strait, Nova Scotia. Atmosphere-Ocean 24 (3), 253–264. https://doi.org/10.1080/07055900.1986.9649250.
Venkatesh, S., El-Tahan, H., Comfort, G., Abdelnour, R., 1990. Modelling the behaviour of oil spills in ice-infested waters. Atmosphere-Ocean 28, 303–329.
Wilkinson, J.P., Wadhams, P., Hughes, N.E., 2007. Modelling the spread of oil under fast sea ice using three-dimensional multibeam sonar data. Geophys. Res. Lett. 34, L22506.
Wilkinson, J.P., Maksym, T., Bassett, C., Lavery, A., Singh, H., Chayes, D., Elosegui, P., Wadhams, P., Evers, K.-U., Jochmann, P., 2014. Experiments on the detection and movement of oil spilled under sea ice. In: Proceedings of the HYDRALAB IV Joint User Meeting, Lisbon, July 2014.
Wilkinson, J.P., Beegle-Krause, C.J., Evers, K.-U., Hughes, N., Lewis, A., Reed, M., Wadhams, P., 2017. Oil spill response capabilities and technologies for ice-covered Arctic marine waters: a review of recent developments and established practices. Ambio 46 (Suppl. 3), S423–S441 2017.
World Meteorological Organization, 1970. WMO Sea Ice Nomenclature. Geneva: World Meteorological Organization. WMO-no 259. TP.145.